Journal of Hydrology 660 (2025) 133438

Contents lists available at ScienceDirect

Journal of Hydrology

journal homepage: www.elsevier.com/locate/jhydrol

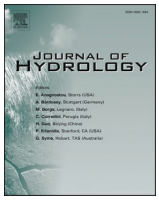

Sensitivity of permissible aquifer recharge rate to hydrogeological and well design parameters

Ranveer Kumar, Anurag Ohri *, Shishir Gaur

Department of Civil Engineering, Indian Institute of Technology (BHU) Varanasi, Uttar Pradesh 221005, India

ARTICLE INFO

This manuscript was handled by Dongmei Han, Editor-in-Chief, with the assistance of Xiaolong Geng, Associate Editor

Keywords:
Permissible Aquifer Recharge Rate (PARR)
Managed Aquifer Recharge (MAR)
Lower Ain River Basin
Sobol' Indices
Recharge Potential

ABSTRACT

The maximum injection rate to an aquifer for a given operational time, hydrogeological and well characteristics, and under the constraints of a permissible head is defined as the Permissible Aquifer Recharge Rate (PARR). A local and global sensitivity analysis (Sobol's Indices) has been presented to address the important hydrogeological and well parameters in determining PARR for confined and unconfined aquifers. A novel methodology to determine PARR for 3D numerical groundwater models has been discussed, and its implementation in Lower Ain Valley has been presented. PARR's sensitivity varies with specific parameter interactions, particularly between hydraulic conductivity and vertical anisotropy in unconfined aquifers, whereas confined aquifers show a broader range of influential factors mainly due to interaction between location of the well-screen and the aquifer parameters. The methodology for determining PARR with an adaptive iteration algorithm based on the analytical solution to the well is more efficient and requires fewer iterations. The Lower Ain Valley reveals significant spatial variability in PARR (22–7.48 $\times$ 10^5 m^3/day) with aquifer characteristics, highlighting the basin's strong aquifer storage potential for addressing severe groundwater deficiencies.

1. Introduction

Groundwater is a critical resource for many communities worldwide, providing a reliable source of drinking water, supporting agricultural and industrial activities, and sustaining ecosystems (Schiff, 1964). The growing demand and the impacts of climate change have placed immense pressure on groundwater resources (Atawneh et al., 2021), resulting in a rapid decline in its storage (Kumar et al., 2024a), and necessitating effective management strategies to ensure long-term sustainability. As natural groundwater recharge has declined due to land modifications, reduced surface water availability (Gaur et al., 2023), Climate and other human-driven factors (Schwartz and Ibaraki, 2011), Managed Aquifer Recharge (MAR) has emerged as a promising approach to enhance groundwater resources and mitigate the impacts of water scarcity (Dillon et al., 2019). MAR can potentially increase groundwater storage, improve water quality, and support local water security (Alam et al., 2021). Many projects for Aquifer Storage and Recovery (ASR) and Aquifer Storage Transfer and Recovery (ASTR) have been initiated all around the world (Dillon et al., 2019) under the cap of MAR, which has emerged as popular water resource management strategy with a total 5 % per year global increase in the number of projects, especially in water-stressed areas of India, US, Europe and Australia (Dillon et al., 2019; Nättorp et al., 2016; Sprenger et al., 2017).

The hydrogeological evaluation necessitates determining the aquifer capacity for assessing site suitability and design recharge rate during the feasibility assessment and conceptual design phase of ASR development (Pyne, 2017). The knowledge of the optimal injection rate during aquifer recharge is vital information required for the site selection, design, and operation of ASR projects (Tiwari and Yadav, 2024). The aquifer storage capacity is the maximum volume of water that can be injected into an aquifer at an optimal rate under the constraint of a permissible head change and operational parameters (well characteristic and Injection duration) (Shandilya et al., 2022a). The aquifer recharge rate through injection wells can be determined using various methods, including temperature-depth profiles (Rushton and Srivastava, 1988), sinusoidal functions (Li et al., 2020), incremental increases in recharge head (Dillon et al., 1994), field tests (Dillon et al., 2019; Martinez and Widdowson, 2023), analytical methods (Shandilya et al., 2022b) and numerical modeling (Kumar et al., 2024b; Tewari et al., 2023). Most recent studies by Shandilya et al. (2022b) demonstrate the determination of aquifer-scale recharge capacity based on analytical solutions for a pumping well in confined aquifers. The methodology

* Corresponding author.
E-mail addresses: ranveerkumar.rs.civ20@iitbhu.ac.in (R. Kumar), aohri.civ@iitbhu.ac.in (A. Ohri), shishirg.civ@iitbhu.ac.in (S. Gaur).

https://doi.org/10.1016/j.jhydrol.2025.133438
Received 26 July 2024; Received in revised form 24 March 2025; Accepted 30 April 2025
Available online 1 May 2025

presented by Shandilya et al. (2022b) does not consider the effect of sources and sinks. Apart from field tests, which are time-consuming and expensive, solutions based on 3D groundwater flow models better represent the real field scenarios than the available analytical solutions, particularly when nearby sources and sinks are present (Myoung-Rak et al., 2020). The current literature lacks the utilization of a numerical groundwater model to explicitly identify the optimal injection rates for both confined and unconfined aquifers.

Kumar et al. (2024) have defined the optimal injection rate under the given operational and geological constraints as the Permissible Aquifer Recharge Capacity (PARC) of an ASR site. They have utilized a linear regression model to determine PARC by mapping the relation between injection rate and head buildup at the grid cells of a numerical model. The method presented is fast and computationally efficient at the expense of the uncertainty raised due to the simplification of the MODFLOW model outputs to a linear response function. In this study, the term "Permissible Aquifer Recharge Capacity (PARC)" has been revised to "Permissible Aquifer Recharge Rates (PARR)" for better alignment with its definition.

The aquifer recharge capacity is highly dependent on the hydrogeological (Transmissivity, Aquifer thickness, Storativity, and Aquifer type) and well characteristics (skin layer hydraulic conductivity, well radius, and well losses) (Hugman et al., 2012; Shandilya et al., 2022a; Tiwari and Yadav, 2024). The effect of well operation parameters (skin factor, wellbore storage, and pumping duration) on pumping capacity has been thoroughly analysed by Shandilya et al. (2022a) with the analytical solution given by Agarwal et al. (1970). The recovery efficiency of an ASR project is highly correlated with the aquifer's transmissivity and thickness (Tiwari and Yadav, 2024). A sensitivity analysis of model parameters is crucial for assessing the significance of model parameters and their uncertainty (Baker et al., 2023; 2022). Sensitivity analysis offers insights into how changes in management practices may affect groundwater resources, enabling informed decision-making (Bianchi Janetti et al., 2019; Reinecke et al., 2019). Based on the current literature, assessing the sensitivity of various decision-making parameters (aquifer and operational) on PARR is essential for its wide application. Local sensitivity analysis deals with the sensitivity of model outputs to small variations in individual input parameters. In contrast, global sensitivity analysis examines the sensitivity of model outputs to the entire range of possible input parameter values (Tang et al., 2007). Since previous literature does not include global sensitivity (Shandilya et al., 2022a), combined local and global sensitivity analyses were performed here to assess the important factors affecting PARR.

One powerful global sensitivity analysis method is Sobol's sensitivity indices, which quantify the contribution of individual input parameters and their interactions to the total variance of the model output (Song et al., 2015). This approach has been widely applied in various fields, including hydrology, environmental modelling, and economic evaluation of healthcare technologies (Bianchi Janetti et al., 2019; Briggs et al., 1994; Gan et al., 2014). Reinecke et al. (2019) found the sensitivity of the simulated head to the aquifer and hydrological parameters of the global gradient-based groundwater model. Tang et al. (2007) compared the performance of Sobol's sensitivity analysis with other popular methods, such as local analysis, regional sensitivity analysis, and analysis of variance, in the context of a rainfall-runoff model and found that Sobol's method yielded more robust sensitivity rankings. The sensitivity of the parameters affecting the PARR is a critical consideration for designing and implementing ASR projects at a site.

In this study, a novel adaptive iteration algorithm has been presented to determine PARR with numerical groundwater flow models to reduce the uncertainty and computational time. The methodology utilizes the analytical relationship between injection rate and corresponding head buildup for confined and unconfined aquifers given by Theis (1935) and Neuman (1972). The factors influencing PARR have been analysed, and their local and global sensitivity has been assessed with Sobol's indices. The implementation of the proposed methodology has been presented for the Lower Ain River Basin, France.

2. Method

A hypothetical homogeneous numerical model for confined and unconfined aquifers has been developed with the representative data presented in Table 1 to demonstrate the proposed methodology and the sensitivity analysis**.** Horizontal anisotropy (HANI) has been defined by the ratio of hydraulic conductivities along the principal horizontal axes. Vertical anisotropy (VANI) has been taken as the ratio of vertical hydraulic conductivity and horizontal hydraulic conductivity along the x-axis. The models have been discretized into ten layers and a varying cell size from 10 m at the injection well (in the center) to 1000 m at the boundaries. The model dimension and boundary conditions have been established such that the influence area of the well never reaches the boundary to avoid sudden head change. The left and right boundaries have been taken as Dirichlet's boundary (specified head), such that a head loss of 5 m occurs from left to right in both cases (i.e. confined and unconfined). The specified head in the case of unconfined aquifer has been set to 55 m on the left and 50 m on the right boundary. The specified head for the confined aquifer is set to 60 m on the left and 55 m on the right boundary. This sets a starting steady state head of 57.56 m at the well location for the confined aquifer and 52.56 m for the unconfined aquifer. The other two boundaries have been taken as no-flow boundaries. Before performing the transient simulation, the steady-state starting head has been established before applying the injection well. The injection well has been modeled with the MNW2 package (Leonard et al., 2009) to control the screen placement and size accurately.

2.1. Permissible aquifer recharge rate (PARR)

2.1.1. Analytical definition

Shandilya et al. (2022a) defined the storage capacity of an aquifer for a given set of operational parameters (duration and well characteristic) as the maximum volume of water that can be injected or extracted under

Table 1
Hypothetical model conceptualization (* for global sensitivity analysis and ** for local and global sensitivity analysis).

	Confined aquifer		Unconfined aqufier	
Properties	Base values	Range	Base values	Range
Dimension	10,000 m × 10,000 m × 50 m	–-	10,000 m × 10,000 m × 60 m	–-
Hydraulic conductivity (H_k)	0.001 (m/sec)	1.15 × 10^{-04}–0.05 (m/sec)**	0.001 (m/sec)	1.15 × 10^{-04}–0.05 (m/sec)**
Specific storage (S_s)/Specific yield (S_y)	1.0 × 10^{-04}	1.0 × 10^{-07}–0.001**	0.2	0.01–0.4**
Horizontal anisotropy (*HANI*)	1.0	0.25–10**	1.0	0.25–10**
Vertical anisotropy (*VANI*)	3.0	1–10**	3.0	1–10**
Well screen length (L_{sc})	50 m (*fully penetrated*)	2–30 (m)*	50 m (*Below the water table*)	2–30 (m)*
Well Screen Location (*Centroid from the bottom of the aquifer*) (H_{sc})	25 m	15–35 (m)*	25 m	15–35 (m)*

the limit of permissible head change. The duration of pumping has been stated as an important factor along with the wellbore storage and skin factor (Martinez and Widdowson, 2023; Shandilya et al., 2022a). Without time constraints, any large volume of water can be stored, even in subpar aquifers, demonstrating the importance of pumping duration in injection well design. The duration constraint is also essential due to the temporal availability of source water for the ASR.

The Permissible Aquifer Recharge Rate (PARR) has been defined as the maximum constant injection rate to an aquifer for a given operational time (and well characteristics) under the constraints of a permissible head (such that PARR × Injection duration = Aquifer's injection capacity).

The head developed due to a constant injection rate manifests a curvilinear shape with a peak at the well itself. The permissible head is required to constrain the head developed near the well to avoid waterlogging or flooding in unconfined aquifers or to prevent the confining layer's failure in confined aquifers (Shandilya et al., 2022b). The constraints imposed by the permissible head near the injection well also limit the storage capacity of the ASR system. As a result, the true capacity of the aquifer cannot be practically utilized by a constant rate of injection (Bergmo et al., 2011). Therefore, the aquifer's injection capacity will be much less than the true aquifer storage capacity. The capacity achieved by the injection will highly depend upon the injection rate, pumping duration, initial head distribution, aquifer characteristics (Shandilya et al., 2022b), and the permissible head.

Fig. 1 illustrates the head developed due to injection with respect to time. The value of PARR has been demonstrated in both analytical solutions (Fig. 1**A**) and hypothetical scenarios affected by periodic groundwater extraction, natural recharge, and evapotranspiration (Fig. 1**B**). The value of PARR is associated with the optimal pumping rate (Q), which generates a head equal to the permissible head (H_{per}) in the injection duration of t_{end}.

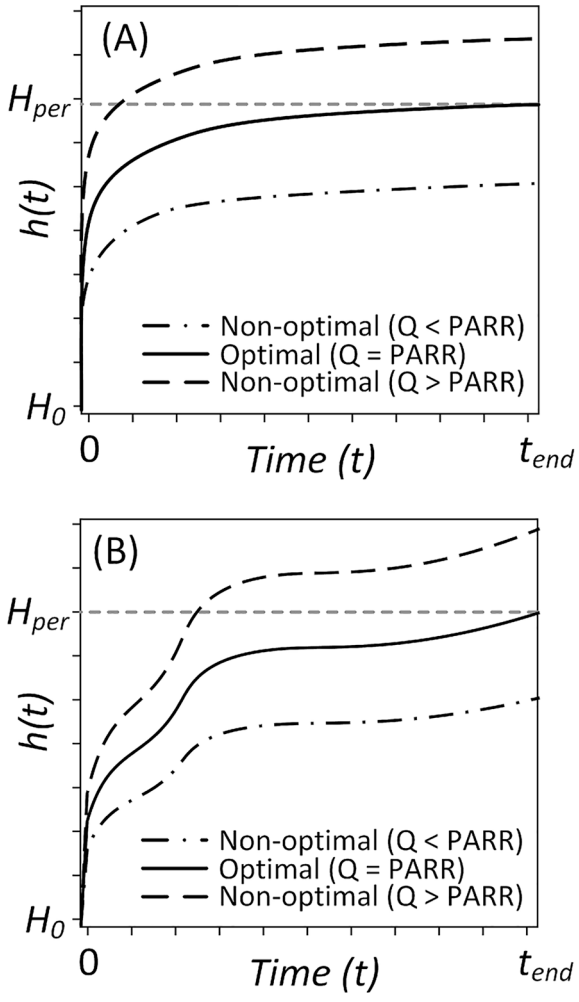

Fig. 1. The definition of PARR as per (A) the analytical solutions (modified from Shandilya et al., 2022a) and (B) the hypothetical field scenario.

The relationship between the recharge rate and the corresponding head development is crucial for the determination of PARR (Kumar et al., 2024b). The analytical solutions for the 2D groundwater flow for pumping/injection wells have been developed by several authors, starting from Dr. C. V. Theis, who assumed the aquifer to be homogeneous and isotropic to an infinite extent (Theis, 1935). The assumption regarding the well losses (i.e. Skin layer effect (Van Everdingen, 1953), wellbore storage (Agarwal et al., 1970), partial well-penetration (Hantush, 1964), unconfined conditions (Neuman, 1972) and inter-aquifer leakages) have been further taken into consideration to refine the Theis' solution. Considering no losses and wellbore storage, the head developed in the well is equal to the head near the well-casing for a fully penetrated case and generally given as.

$$h = h_0 + \frac{Q}{4\pi T} W(u) \tag{1}$$

Where h_0 and h are the initial head and head at time t, respectively. Q is the pumping/injection rate, and T is the transmissivity of the aquifer. The $W(u)$ is the function of one or several parameters depending on the well characteristics and aquifer type, generically known as the well function (Neuman, 1972; Theis, 1935). If $W(u)$ does not depend on the Q (i.e., neglecting the nonlinear head loss) for a given pumping duration, the value of $W(u)$ is constant at a fixed radial distance (r) from the well. Therefore, the optimal water injection rate ($PARR$) is determined such that the injected volume is maximized while ensuring that the head near the well ($r = r_w$) at the end of injection ($t = t_{end}$) equals the permissible head (H_{per}).

$$PARR = \frac{4\pi T.(H_{per} - h_0)}{W|_{r=r_w, t=t_{end}}} \tag{2}$$

2.1.2. Numerical solution

Since the analytical 2D solution to the well does not consider the effect of nearby sources and sinks (Freeze and Cherry, 1979), it is imperative to utilize 3D numerical models to determine the aquifer scale recharge capacity, especially for a complex groundwater system. Numerical groundwater models (such as MODFLOW) have been utilized in many projects worldwide due to their versatility and accuracy in complex studies (Freeze and Witherspoon, 1966; Kuiper, 1983), following advancements in computing power. Due to the forward modelling approach of MODFLOW, the direct determination of PARR is impossible and hence requires an iterative method to find the optimum solution. The forward simulation determines the heads with given stresses and boundary conditions in a numerical groundwater model. A simple optimization approach is generally needed to determine the PARR by maximizing the net injected water volume for a given injection duration.

$$maximise(Q_i \times t_{end})$$

$$S.T.\left(h_{i,t}|_{Q=Q_i,\, t=t_{end}} - H_{per}\right) \leq \epsilon \tag{3}$$

Where Q_i represents the injection rate [L^3T^{-1}] at location i, $h_{i,t}$ is the simulated head [L] with Q_i at the end of the injection duration (t_{end})[T], and ϵ is the tolerance limit [L] which is the acceptable difference between actual permissible head and simulated head at the end of injection.

Since the head varies monotonically with time, the optimization method eventually converges to the maximum recharge rate, creating a head equal to H_{per} at $t = t_{end}$. The optimization method can be time-consuming with a numerical model, especially with real-field complex

models. The number of iterations required to find the optimum solution in groundwater problems often depends on the choice step size. Selecting an optimal step size is crucial; a step too small may result in slow convergence, whereas a step too large could lead to oscillation around the minimum or divergence of the loss function (Ruder, 2017). The dynamic step size based on known properties of the objective function, such as the relation between recharge rate and corresponding head change, can help address this issue (Tholeti and Kalyani, 2020). We devised an adaptive iteration algorithm that computes PARR using a linear relation of injection rate and head developed, requiring minimal additional computation compared to gradient descent (Zeiler, 2012). Given that $t = t_{end,}$ and $r = r_w$, i.e., at a particular injection duration and at a fixed distance from the well (in this case equal to the radius of the well (r_w)), the value of the well function becomes constant, and the Eq. (1) becomes linear (Fig. 2).

$$Q_i = C_1 - C_2 h_{i,t} \text{ where } C_1 \text{ and } C_2 \text{ are constants} \quad (4)$$

After simulating the model with a selected upper and lower bound of Q_i, which are used to determine the *C1* and *C2* in Eq. (4), we utilized the linear relationship to determine the first estimate of PARR. The constraint of the maximum head simulated at the end of the injection is checked with the permissible head. The estimated PARR is accepted if the residual is within the tolerance limit. The tolerance limit controls the number of iterations required to determine PARR. A lower value will yield more accurate estimation while requiring more iterations. During the implementation of the proposed methodology, it has been observed that in the case of a confined aquifer, it took only 3–12 iterations to determine PARR with a tolerance of 1 cm. However, In the case of an unconfined aquifer, the number of iterations required was in the range of 8–56.

In the case of unconfined aquifers, the relation between Q and h is nonlinear (Martinez and Widdowson, 2023), i.e., the calculated maximum head corresponding to the initial estimate of PARR can be lower or higher than the permissible head. The upper or lower bound is updated with the estimated Q, depending upon the residual characteristic. The linear relationship is fitted again to find the next Q value corresponding to H_{per}. Since the relation between the head and the injection rate is monotonously increasing, the algorithm converges faster with the dynamic step size. The method has been presented in Fig. 3.

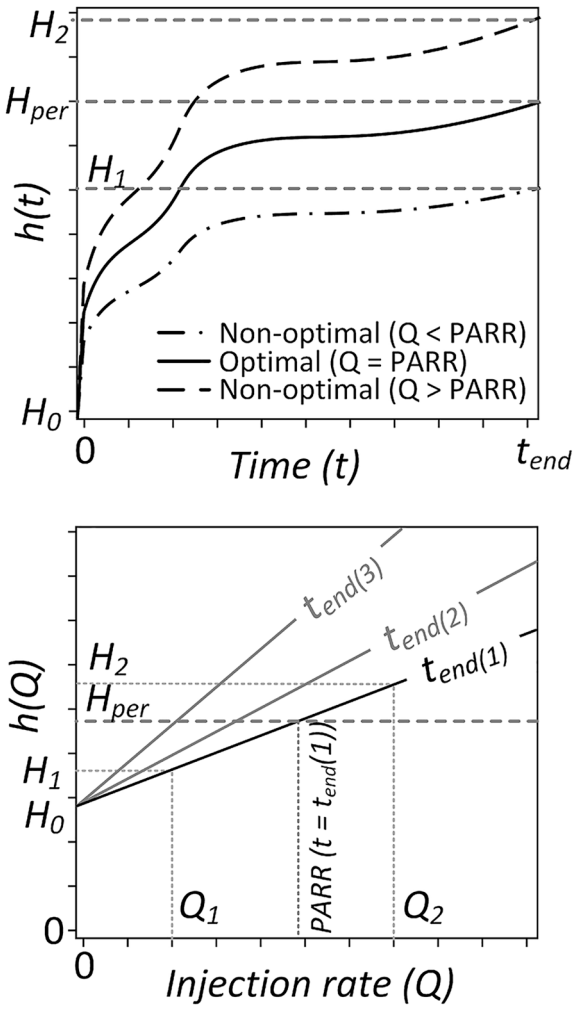

Fig. 2. The determination of PARR with simulated heads (The linearity between h and Q for a given injection duration is shown in the figure on the left. The slope of the h vs Q curve depends on the injection duration.).

2.2. The permissible and recoverable head

As the water is injected into the aquifer with a constant recharge rate, the head rises near the screen and propagates towards the confining layer or water table (Welch et al., 2013). The pressure head developed near the confining layer at the critical location (mainly near the injection well) can rupture the confinement of confined aquifers or raise the water table to cause flooding in unconfined aquifers. The permissible head (H_{per}) refers to the maximum allowable pressure head that can be achieved at the injection site without inducing any adverse effects. The difference between the initial and permissible head is termed the recoverable head ($H_{per}-h_0$) and is an essential criterion in determining PARR. The larger recoverable head represents the more significant groundwater deficiency, resulting in a higher value of PARR and vice versa.

The rupture of the confining layer is controlled by limiting the head built up near the critical location below the safety limit of overburden pressure in the case of confined aquifers (Parker et al., 2022). For a geological layered system with minor principal stress oriented in the horizontal direction, the permissible head for a confined aquifer is given as (Shandilya et al., 2022b).

$$H_{per} = h_o + h_{fp}(1 - SF) \quad (5)$$

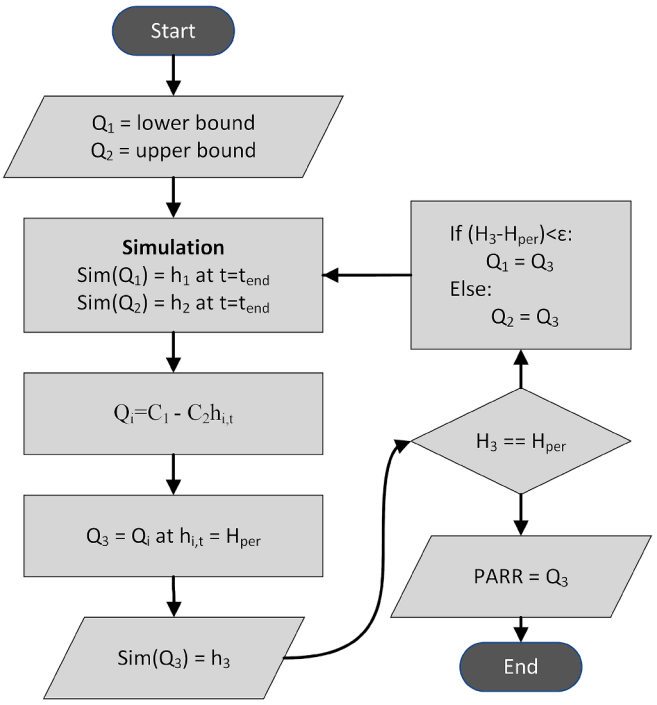

Fig. 3. Flow chart for the calculation of PARR with MODFLOW simulation.

Where H_{per} is the permissible head [L], h_0 is the initial head [L], h_{fp} represents the fracture pressure head of the confining layer [L], and *SF* is the factor of safety.

In the case of an unconfined aquifer, the allowable head is constrained by the chance of flooding or generation of artesian conditions in the vicinity of the injection well. The permissible head is selected based on site-specific conditions, such as avoiding the rootzone depth in the agricultural area or the foundation depth of the building in a residential area and government norms (Shandilya et al., 2022b).

3. Results and discussion

3.1. PARR and recoverable head

The PARR for the base conditions (Table 1) with a varying injection duration (*from seconds to Months*) has been determined using the presented methodology. The permissible head for the given conceptual model in the case of an unconfined aquifer is taken as 57 m (3 m *below ground level (mbgl)*) and 90 m for a confined aquifer (*arbitrarily taken to represent a hypothetical overburden layer*). The recoverable head for the hypothetical unconfined aquifer was 4.44 m (H_{per} = 57 m and h_0 = 52.56 m), and for the hypothetical confined layer, it was 32.44 m (H_{per} = 90 m and h_0 = 57.56 m). The PARR has been presented with respect to unit recoverable heads to make the results comparable between confined and unconfined aquifers.

The PARR values are initially high for short injection durations and decrease over time (Fig. 4**A**). This trend reflects the decrease in the injection rate required to reach the permissible head as the duration increases. In the unconfined aquifer, the decline in PARR with respect to the t_{end} is initially steep, which further attenuates.

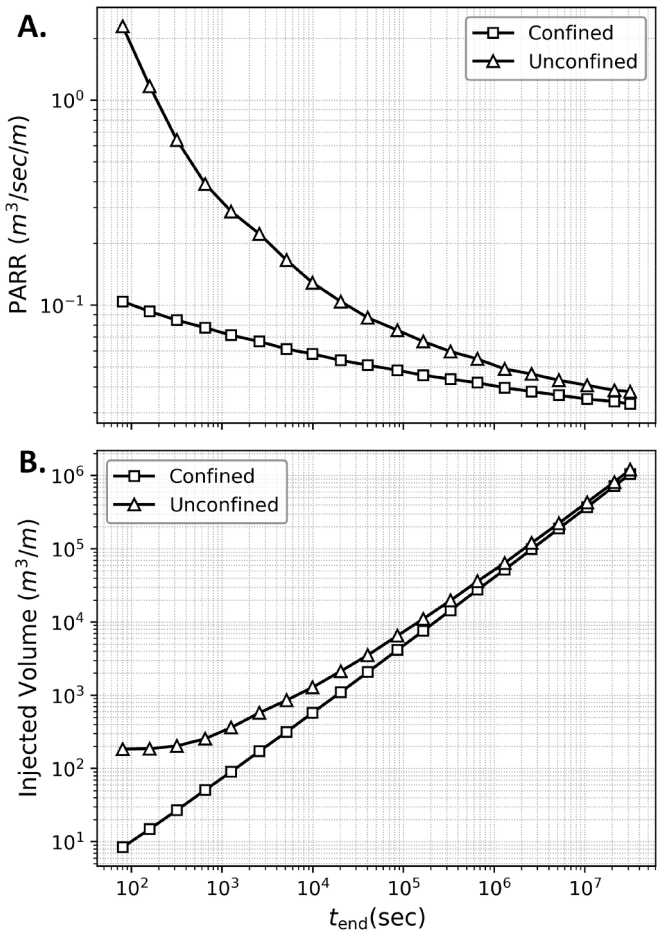

Fig. 4. (a) variation of PARR per unit recoverable head w.r.t injection duration and (b) The injected volume per unit recoverable head corresponding to the PARR.

For shorter injection durations, the unconfined aquifer exhibits significantly higher PARR values—approximately 14 times greater than those observed in the confined case. However, as the injection duration increases, the difference between the two cases diminishes, following a general power-law relationship. This behaviour is attributed to the distinct hydrodynamic responses of confined and unconfined systems. In unconfined aquifers, delayed gravity drainage affects the rate of head decline (Freeze and Cherry, 1979). The initial condition of the water table and the effects of gravity drainage led to a rapid initial rise in the head, which is then moderated over time (Huang et al., 2019), resulting in a steep decline in the PARR for short durations.

The maximum volume injected within the constraint of permissible head and duration is called the aquifer's injection capacity (Shandilya et al., 2022a). The injection capacity was calculated by multiplying the PARR with the injection duration, presented in Fig. 4**(b)**. For the confined aquifer, the injection capacity per unit recoverable head increases sub-linearly with respect to the injection duration, indicating a steady accumulation of injected volume. In contrast, the unconfined aquifer initially exhibits a slower rate of increase, reflecting the delayed propagation of pressure and groundwater head buildup. This is likely due to the gradual rise of the water table, which influences the effective storage characteristics of the system (Welch et al., 2013).

The injection capacity in the unconfined aquifer accelerates with t_{end}, reducing the difference between the two cases. For longer injection durations ($t_{end} > 10^5$ sec), the injection capacity curves for both aquifers become nearly parallel, indicating that the influence of initial transient effects in the unconfined case diminishes. This suggests that, at large time scales, the storage behaviour of confined and unconfined aquifers becomes more comparable.

3.2. Local sensitivity analysis

3.2.1. Effect of aquifer parameters on PARR

The characteristics of the aquifer, such as hydraulic conductivity and storage coefficient, play a vital role in determining the maximum injection rate under the allowable constraints (Shandilya et al., 2022a). The effect of aquifer hydraulic conductivity (H_k), specific storage (S_s), horizontal anisotropy (*HANI*), and vertical anisotropy (VANI) has been analysed and presented for four injection durations (1 hr, 1 day, 1 month, and 1 year). The representative value range of aquifer parameters has been taken to analyse the PARR's local sensitivity and tabulated in Table 1. The value range has been chosen to represent the general characteristics of the aquifer and the constraints of screen length (L_{sc}) and centroid location (H_{sc}) based on aquifer dimensions. The L_{sc} is set at 50 m for confined and unconfined conditions, representing a fully penetrated well in the base scenario. Given the assumed 50 m thickness for confined aquifer and 52.56 m saturated thickness for unconfined aquifer, L_{sc} has been limited to a maximum of 50 m length. By varying L_{sc} between 2–30 m, we create adequate space and enable H_{sc} to vary between 15 m and 35 m, remaining within the aquifer/saturated thickness.

The PARR has shown a nonlinear relation with the aquifer parameters, and the slope of the curve depends on the duration of injection. The variation of PARR with respect to aquifer and well parameters has been plotted in Fig. 5 and Fig. 6. It should be noted that although the fitted curve appears linear for a large injection duration, it is actually nonlinear.

In the case of the confined aquifer, the PARR is non-linearly correlated to the H_k (fitted to the polynomial function of 2nd order) and shows high sensitivity (Fig. 5**(1A)**). As H_k increases, the head developed for the given injection rate decreases, resulting in a high injection rate to reach the H_{per}. For a longer duration, the fitted curve between H_k and PARR tends to become linear. The PARR increases with S_s with a large gradient for $S_s < 0.00012$ and further with a lower gradient after S_s

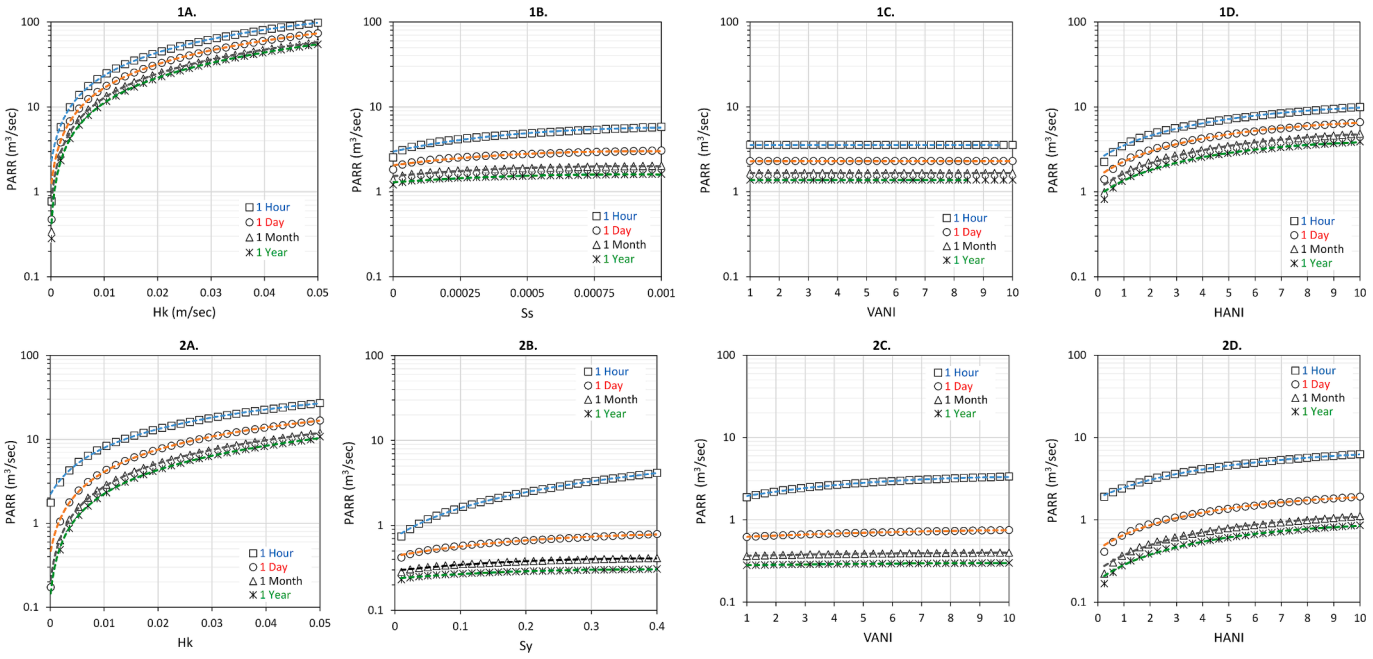

Fig. 5. The local sensitivity of PARR with aquifer parameters in the (**1**) confined aquifer and (**2**) unconfined aquifer (**A**.linear plot between PARR and H_k; **B**. linear plot with respect to S_s or S_y; **C**. linear plot with respect to VANI and **D**. linear plot with respect to HANI).

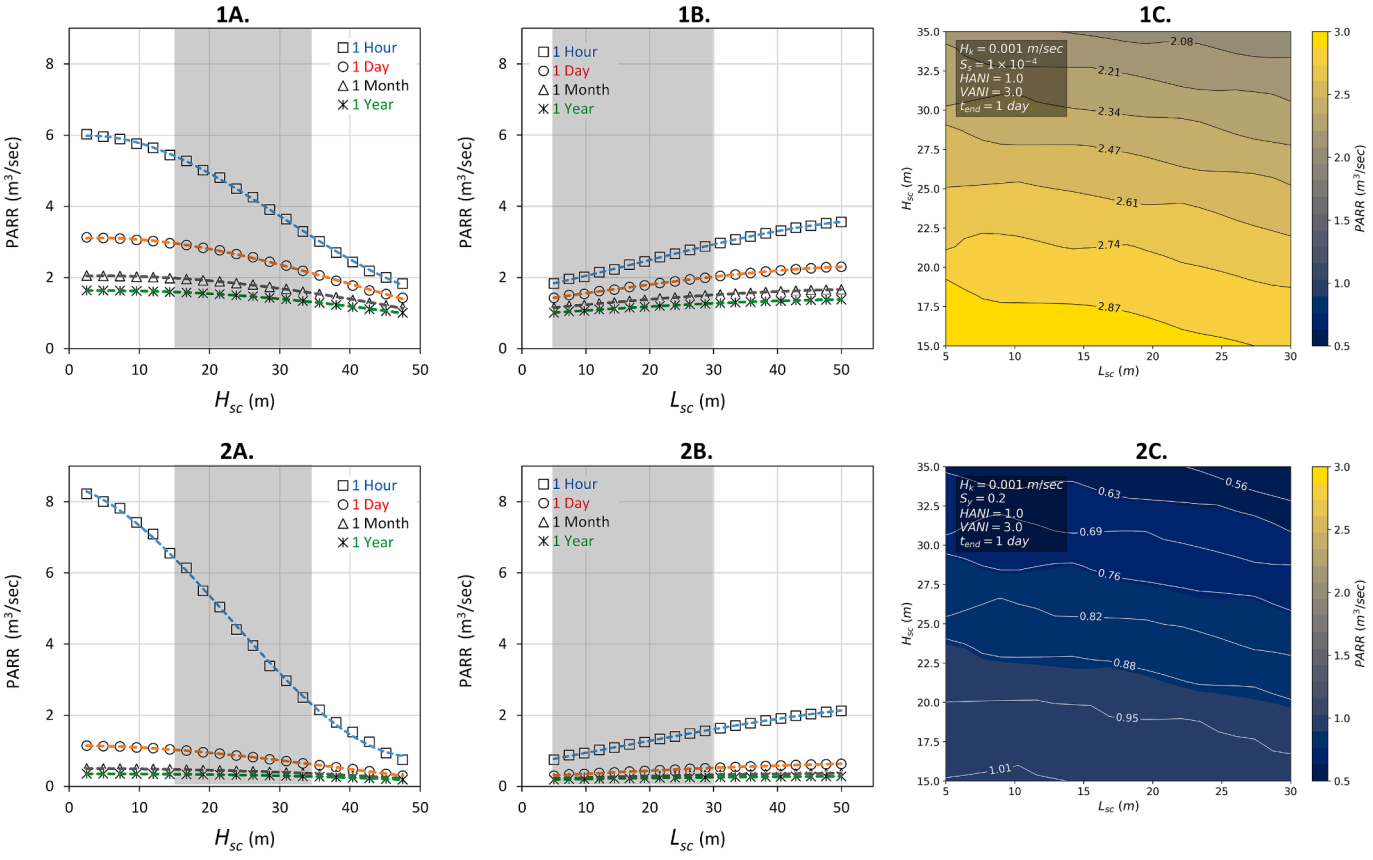

Fig. 6. The variation of PARR with respect to well characteristic in (**1**) confined aquifer and (**2**) Unconfined aquifer (**A**. with respect to screen location (H_{sc}) (the location of the centroid of the screen is varied from bottom to the aquifer/saturated thickness with L_{sc} = 3 m) **B**. with respect to screen size (L_{sc}) (L_{sc} has been increased from top of the aquifer towards bottom starting from 5 m to 50 m such that the top elevation is fixed (H_{sc} = 47.5 m to H_{sc} = 25 m)) and **C**. contour plot depicting the combined effect of screen size and location within the shaded parameter space).

≈0.00012 (Fig. 5**(1B)**). The PARR for the fully penetrated well in the confined aquifer is insensitive to *VANI* as it shows insignificant variation (Fig. 5**(1C)**). It is consistent with the assumption of radial flow in a fully penetrated confined aquifer (Theis, 1935). The increased horizontal anisotropy results in high conductivity in one of the horizontal principal planes, necessitating a high injection rate to achieve head rise and vice versa. This results in a higher value of PARR (Fig. 5**(1D)**); hence, PARR shows considerable sensitivity to *HANI*.

The PARR also varies non-linearly with H_k for the unconfined aquifer (Fig. 5**(2.A)**) and has been fitted with the polynomial function of 2nd order. The PARR also shows polynomial variation with S_y and has a higher gradient for the smaller duration of injection (Fig. 5**(2.B)**). The gradient attenuates for a higher injection duration. The PARR is sensitive to the vertical anisotropy (*VANI*) in the case of an unconfined aquifer and can be fitted by 2nd order polynomial function (Fig. 5**(2.C)**). The sensitivity of PARR to *HANI* again follows the polynomial function with a high gradient (Fig. 5**(2.D)**).

3.2.2. *Effect of location and length of well screen on PARR*

The analytical solution for the head dissipation by Jenkins et al. (2019) suggests that the dissipation of the head raised due to water injection into the aquifer depends on the time and aquifer conductivity. The time required for the head to propagate to the top of the aquifer (i.e., at the critical location) is inversely related to the aquifer's vertical conductivity (Welch et al., 2013). It makes the starting location of head propagation or the location of initial fluid potential (Freeze and Cherry, 1979) important for determining PARR since the time required for the head to propagate to the critical point in the case of a confined aquifer and the water table in the case of an unconfined aquifer depends on the starting location. This elapsed time contributes to the delayed response of injection to the head at the critical point (Neuman, 1972), leading to high PARR values for shorter injection durations. The phenomenon is more prominent in the case of aquifers with significant thickness, where a fully penetrated well is not feasible. The partial penetrating well leads to a vertical component of groundwater flow near the well in the case of the confined aquifer, which was insensitive to the vertical anisotropy in the case of a fully penetrated well. It raises a decision-making problem for the well-screen location in the aquifer.

It is clear that the sensitivity of PARR to both the screen's centroid position from the bottom of the aquifer (H_{sc}) and size (L_{sc}) primarily depends on the distance from the point of head propagation, which refers to the location of the top of the screen. This perspective assumes an even distribution of the head across the length of the screen. The sensitivity of PARR to H_{sc} and L_{sc} provides insights for determining suitable screen size and location within the aquifer. The PARR has been determined by varying the screen size from the top of the aquifer. The effect of screen location on PARR has been analysed by changing the H_{sc} from the bottom of the aquifer while keeping the L_{sc} fixed at 3 m. It should be noted that while the screen length is varied, the value of H_{sc} also varies. Therefore, the combined effect of L_{sc} and H_{sc} on PARR has also been presented in Fig. 6(1C & 2C).

The PARR increases with increasing distances from the critical point in confined aquifers, as well as from the water table in unconfined aquifers. Therefore, when varying the H_{sc} from the bottom towards the critical point, the PARR decreases with increasing H_{sc} for confined and unconfined aquifers for all injection periods. The variation shows an excellent fit with the 3rd-order polynomial equations with high R^2 values (Fig. 6(1A & 2A)). The trends show the most significant change occurring within the first hour (i.e., *small duration*) and the least significant over a year (i.e., *long duration*).

The variation of PARR with L_{sc} also depends upon the location of the screen. As the screen is placed on the top aquifer, where the critical location exists, the PARR increases as the L_{sc} increases. However, if placed at the bottom of the aquifer, the value of PARR decreases as L_{sc} increases. It is essential to understand that the method of varying the L_{sc} affects the local sensitivity of PARR to L_{sc}. To avoid confusion, it is more effective to understand this variation in terms of the distance between the centroid of the well screen and the critical point. In Fig. 6**(1B & 2B)**, the L_{sc} is increased from the top of the aquifer downward while maintaining a fixed upper end. This adjustment results in a greater distance from the centroid of the well screen to the critical point, which, in turn, leads to an increase in PARR. The 3rd-order polynomial function properly explains the variation. Similar to H_{sc}, the most significant variations occur within the first hour and the least significant over a year (Fig. 6**(1B & 2B)**).

In the case of an unconfined aquifer, the water table build-up occurs due to mass balance rather than a change in pressure. The injected water creates the head mound, which is continuously propagated in the radially outward direction, resulting in a continuous increase of influence area (Chahar, 2015). Neuman (1972) derived an analytical solution to map the delayed response of the unconfined aquifer to pumping/injection. The water table rises at a lower rate in the unconfined aquifers when compared to Theis' solution (Confined aquifer) (Freeze and Cherry, 1979; Freeze and Cherry, 1979). When the screen size varies from the bottom, large values of PARR are observed, which decrease as the top of the screen approaches the saturated thickness.

In Fig. 6, plots 1C and 2C provide a detailed visualization of how the parameters H_{sc} and L_{sc} jointly influence the PARR. The parameter space in the plot 1C and 2C has been taken as per Table 1 to avoid non-physical scenarios by satisfy the constraint of $L_{sc} \leq 2 \times minimum\ \{H_{sc},\ 50\text{-}H_{sc}\}$. This constraint ensures that the screen remains within the aquifer thickness/saturated thickness. In both contour plots, it is evident that PARR values are highest when H_{sc} and L_{sc} are minimum and vice versa. It was found that the head attenuation caused by screen location was higher than by screen size when determining PARR. Since PARR is more sensitive to the screen location than size, the screen should be placed near the bottom of the aquifer in case of partial penetrating well. The screen size is a design problem of the well and requires an assessment of head losses caused by higher exit velocity. This has been discussed by (Pyne, 2017) and (van Lopik et al., 2021) in detail.

3.3. *Global sensitivity analysis*

The aquifer's response to injection is complex, depending upon multiple aquifer and operational parameters. The conventional approach of local sensitivity analysis (Shandilya et al., 2022a; Wang and Luo, 2021), which evaluates the impact of individual parameters, may not be sufficient to capture the combined effects of multiple parameters on the system response. Performing global sensitivity analysis can help identify the most influential parameters that control the model outputs. Sobol's method is a widely used global sensitivity analysis technique that can decompose the variance in model outputs into the contributions from individual parameters and their interactions (Andrews, 2008). It has been widely applied to environmental models to assess the impact of parameter uncertainty on model predictions (Nossent et al., 2011). In our study, we adopted Saltelli's modified Sobol method (Please refer to Appendix A) to accurately calculate the first-order, second-order, and total-order sensitivity indices, providing a detailed understanding of the influence of each parameter on the model output. The SALib library by Herman and Usher, (2017) in Python was used to determine the sensitivity of PARR to different aquifers and well parameters with Sobol's indices. The three Sobol indices viz 1st order (S1), 2nd order (S2), and total index (ST) have been computed and presented in Fig. 7. The 2nd-order Sobol's index represents the interaction between two parameters and has been represented in Fig. 7(1B and 2B).

The sensitivity of PARR has been determined to the four aquifer parameters (1. Hydraulic conductivity (H_k), 2. Storage coefficient (S_s or S_y), 3. Vertical anisotropy (*VANI*), and 4. Horizontal anisotropy (*HANI*)) and two well parameters (1. Well screen size (L_{sc}) and 2. Well screen location (H_{sc})). The t_{end} is also a sensitive parameter in the determination of PARR and has been analysed by Shandilya et al. (2022a). In this paper, tend has been taken as one day for the global analysis with

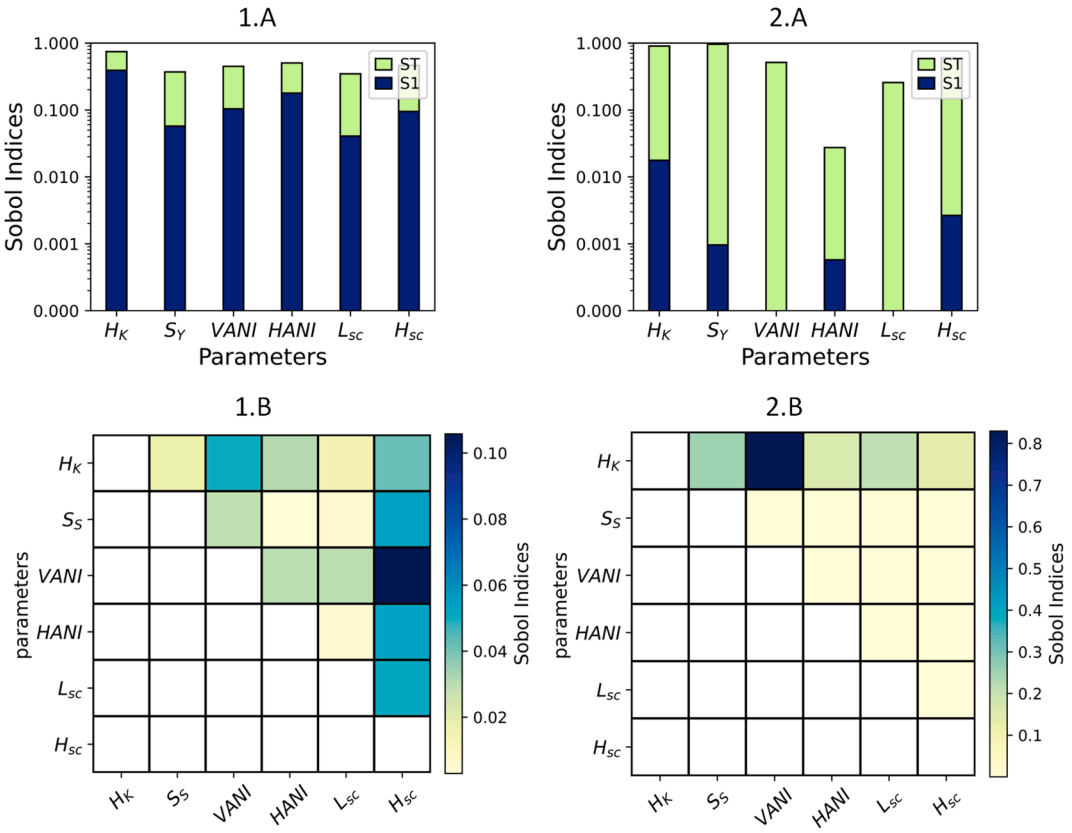

Fig. 7. 1A-1B. Sobol Indices S1, ST, and S2 for PARR in the confined aquifer; **2A-2B**. Sobol Indices S1, ST, and S2 for PARR in unconfined aquifer.

Sobol's method. The parameter space has been taken as per the Table 1.

For the confined aquifer, all parameters (H_K, S_Y, *VANI, HANI,* L_{sc}, H_{sc}) have high first-order sensitivity indices (S1), indicating that each parameter strongly affects the output variance. The sensitivity of VANI has not been apparent during the local sensitivity analysis due to the fully penetrating well. The S1 highlights the effect of partial penetrating well on the sensitivity of PARR to VANI. The total sensitivity indices (ST) are higher than the first-order indices, suggesting high parameter interactions. The interaction effect between pairs of parameters by S2 indicates that all the parameters' pairs significantly affect the sensitivity. The interaction between *VANI* and H_{sc} is the most significant, indicating a strong dependency between these two parameters Fig. 7 **(1B)**. Apart from this, H_{sc} shows significantly high parameter interaction with all the parameters, showing the importance of partial penetrating well on the aquifer capacity.

In the case of an unconfined aquifer (Fig. 7**(2A)**), all the parameters have high total sensitivity except *HANI*, although it still contributes through interaction. The first-order index is relatively lower compared to confined aquifers. The *VANI* and L_{sc} have the lowest S1 values, which implies that the direct influence of these parameters on the PARR is less, and the sensitivity relies on the interactions. The H_k, S_y, and H_{sc} have higher direct and total contributions.

The parameter H_k interacts significantly with *VANI* in both aquifer types, indicating that hydraulic conductivity and vertical anisotropy are closely linked in their influence on PARR. The unconfined aquifer shows higher interaction effects for the pair H_k and *VANI* than the confined aquifer. In the confined aquifer, H_k interacts more broadly with multiple parameters (*VANI, HANI,* L_{sc}), suggesting that the influence of hydraulic conductivity is distributed among several parameters. In the unconfined aquifer, the interactions are more concentrated, with the most substantial interaction being between H_k and *VANI*. The confined aquifer exhibits stronger second-order interactions between specific parameter pairs, indicating that parameter combinations have a more pronounced effect on the PARR, potentially due to the confined nature restricting flow and increasing dependency on specific parameters (Shandilya et al., 2022a; Sun et al., 2018). The phenomenon is justified by the response of the aquifer to pumping, where the pressure drops lead to drawdown, affecting how quickly water can be replenished from surrounding areas, which essentially depends upon the hydraulic parameter combination (Chahar, 2015; Houben, 2015). The interplay between the pressure head and the aquifer's hydraulic properties (Pyne, 2017) means that parameter combinations have amplified effects on PARR due to these dynamic responses.

3.4. PARR for site selection

The suitability of a location for the ASR project mainly depends on three factors: (a) the deficiency of groundwater, (b) the availability of a transmissive aquifer, and (c) the availability of water for injection. The PARR satisfies the first two parameters, as it depends on the aquifer parameters and the recoverable head. It accurately delineates suitable water injection locations in the aquifer (Kumar et al., 2024b). The water availability is subject to the source of water selected for the injection. The storm runoff in excess of the water demand (surplus water) in the area can become a vital source for injection. The suitability of an area for ASR projects can be assessed based on the availability of water and PARR, and the detailed subbasin scale methodology can be found in Kumar et al. (2024b). The injection operation can be optimized using PARR for the storm generation and accumulation period. It will create a buffer recharge for the dry period in semi-arid regions for sustainable groundwater management.

4. Implementation

The application of the presented methodology has been demonstrated in the groundwater model of Lower Ain Valley, France. The river

has been extensively studied for its connectivity to the groundwater (Bajpai et al., 2023; Gaur et al., 2011; Graillot et al., 2014; Lejot et al., 2007; Mishra et al., 2023). The Ain, having an oceanic hydrologic regime, is 200 Km long and drains over 3713 Km^2 of the Jura Mountains to the Rhône River (Olivier et al., 2009). Recent summer droughts of 2022 in France due to unusual weather have resulted in reduced groundwater levels and stream discharge (Corne, 2023). The assessment of climate change's impact on future groundwater with the historical reference period (1976–2005) shows an increase in wetter/drier groundwater extremes (Vergnes et al., 2023). To mitigate this extreme effect of drier groundwater during summer, the ASR system can be a viable solution, storing excess water during wetter events. The PARR of the Ain River basin can be valuable data for assessing ASR feasibility in the area.

4.1. The groundwater model and determination of PARR

The groundwater model of the study area has been developed by Bajpai et al. (2023), and a detailed modelling process, along with calibration and validation, has been explained for reference to the readers. The basin comprises an unconfined aquifer containing highly conductive gravel in the alluvial zone of the Ain River, underlain by fine glacial sediments. The aquifer properties have been presented in Fig. 8. The area has been modelled with 250 m square grids and two layers in MODFLOW-2005. Two boundary conditions (no-flow and specified flow boundary) were used to define the model domain Fig. 8**(A)**. The inflow and outflow flux has been calculated by the observed groundwater heads using Darcy's flux. The Ain River is modelled as the head-dependent boundary with the stream package (STR1).

The PARR in the study area has been determined using the numerical model as well as with unsteady state analytical solution to well in the unconfined aquifer (as discussed in Section 2.1.1). The WTAQ (Barlow and Moench, 1999) computer program was used to determine the analytical value using a Python wrapper. The WTAQ is a freely accessible program to simulate axial-symmetric flow to a well in a confined or unconfined aquifer. WTAQ is based on the analytical model developed by (Moench, 1997). This model determines the axial-symmetric flow to a partially penetrating, finite-diameter well that pumps water from a homogeneous, anisotropic aquifer in confined and unconfined aquifers. The injection well in the numerical model has been simulated with the MNW2 package in MODFLOW (Leonard et al., 2009). The MNW2 package simulates the wells by incorporating the head loss due to well characteristics and aquifer formation. This results in more accurate head estimation in cells with respect to the standard well package. A dummy injection well with a radius of 12.7 cm and a screen length of 6 m was set up in each location (in each grid of the groundwater model and at each data point in the datasets on 30 m resolution) one by one, with the well screen situated at one meter above the aquifer bottom. The permissible head has been taken as 3 m below ground, and the pumping duration is 1 year. The data for the analytical solution has been prepared in QGIS with borehole logs, water table, and pumping test data available at BRGM (Bureau de Recherches Géologiques et Minières) (Fig. 8).

4.2. PARR in Lower Ain Basin

The groundwater levels on the left of Ain River are sufficiently near the ground, resulting in lower recoverable head Fig. 8**(G)**. The lower elevation alluvial plain near the Ain River has the water table above the permissible head, and PARR has not been calculated in this area (represented as the balanced area in Fig. 9). Apart from this, the boundary and stream cells have not been included in the determination of PARR. The distribution of PARR in both cases has been presented in Fig. 9(a and b).

The groundwater head in any area depends on the seasonal variation of natural recharge and discharge by sinks (such as pumping wells and streams). This variation is essential, where the developed built-up head forms the significant criteria in the determination of PARR. This is evident by the comparative assessment of PARR determined by a numerical model (which incorporates all the sources and sinks in the area) and an analytical model (Fig. 9). The numerical solution of PARR in Ain

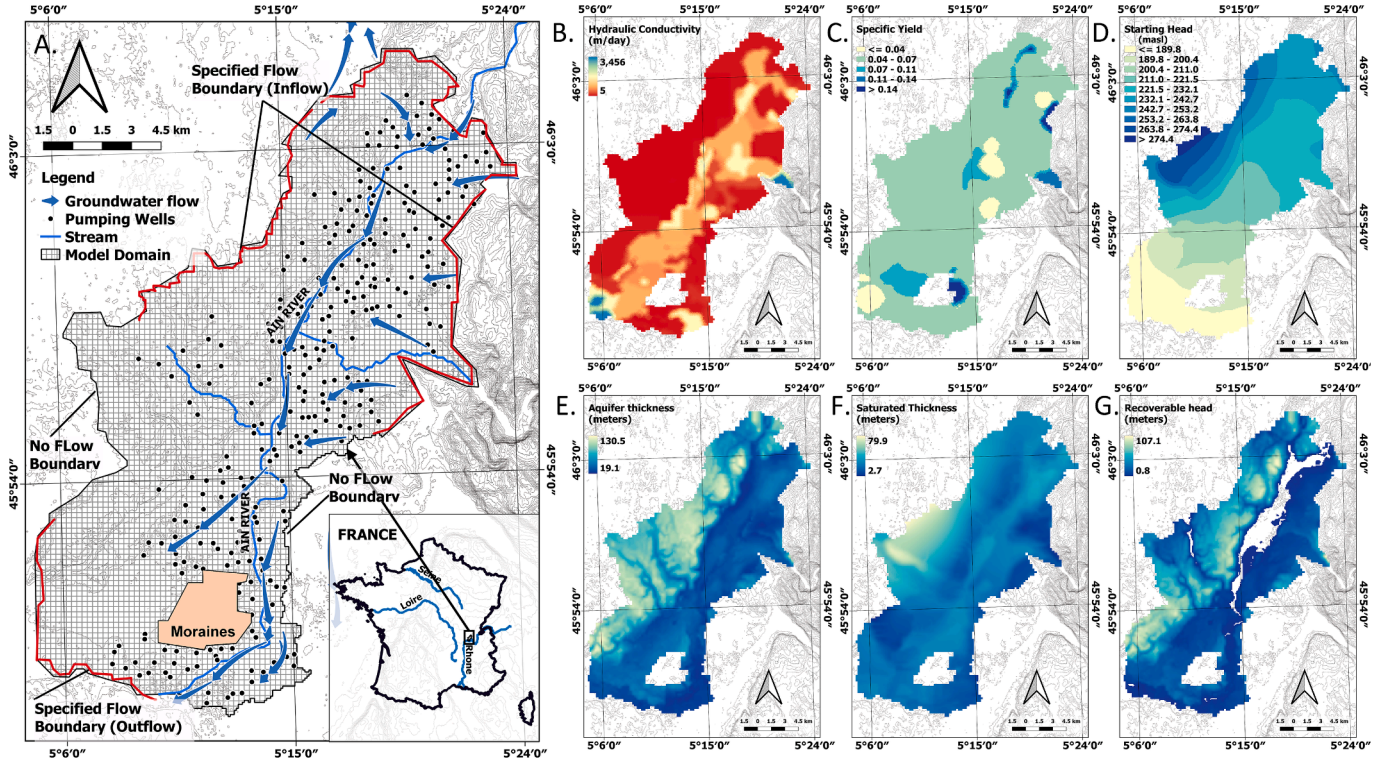

Fig. 8. A. Conceptual groundwater model of Lower Ain River Basin, B. Hydraulic conductivity, C. Specific Yield, D. Initial water table contours, E. Aquifer thickness, F. The saturated aquifer thickness and G. Recoverable head.

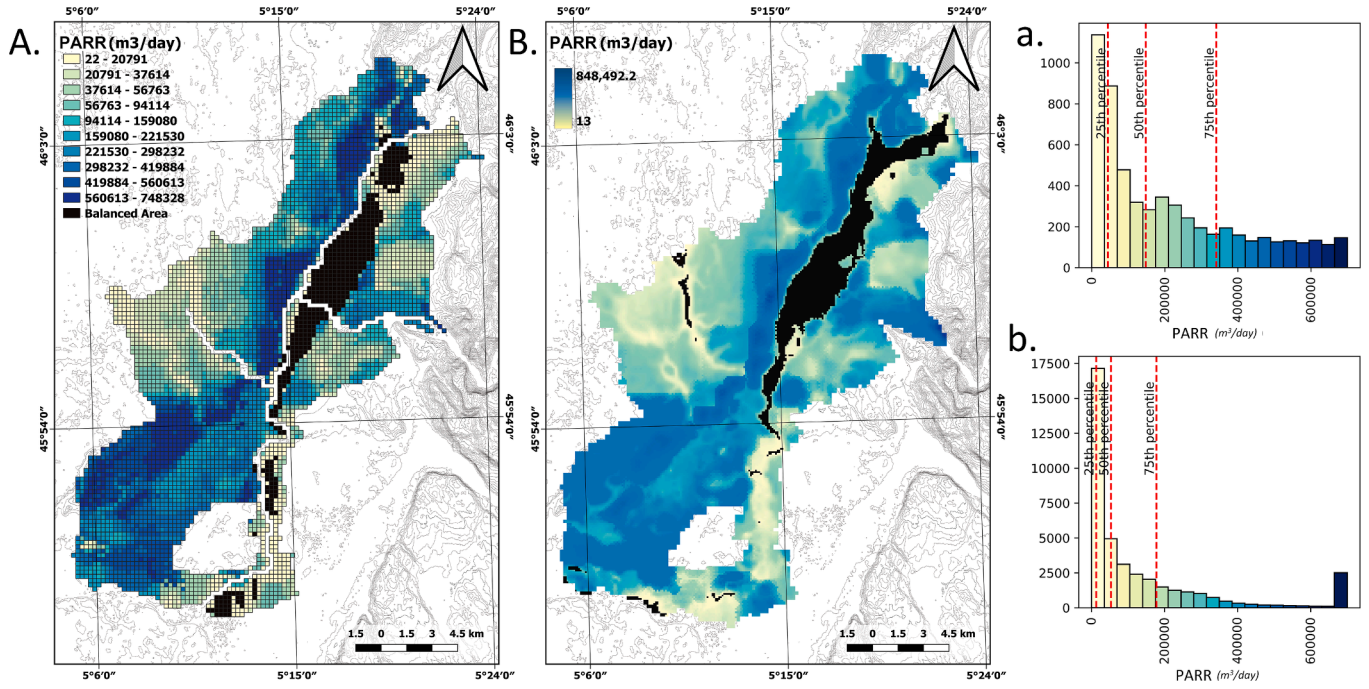

Fig. 9. **A**. PARR determined with MODFLOW model, **B**. PARR determined with analytical method; (**a**. histogram of PARR determined with MODFLOW and **b**. with analytical method).

shows a variation from 22 m^3/day to 7.48 $\times$ 10^5 m^3/day, while it ranges from 13 m^3/day to 8.48 $\times$ 10^5 m^3/day for the analytical method. Apart from the range, the three quantiles of the PARR values are much higher for the numerical solution (Fig. 9(a and b). This shows that the analytical solutions under-determine the PARR due to the non-consideration of sources and sinks.

The hydraulic conductivity is the most sensitive parameter, and the spatial distribution of PARR follows the hydraulic conductivity in the study area. The alluvial plain on the right has high hydraulic conductivity as well as a recoverable head, which results in the highest PARR values. The locations near Ain River would not be very suitable for managed aquifer recharge since the proximity to the river and high aquifer transmissivity can reduce the recovery efficiency. The area right of the moraines is well suited due to sufficient distance from the Ain River and high PARR values.

5. Limitations and future scope

The study presented has some limitations due to assumptions made during the calculations of PARR. The first set of uncertainties comes due to the numerical approach. For a localized study of PARR, the 2D analytical solution of flow to the well (Neuman, 1972; Theis, 1935) will provide accurate results (Anderson et al., 2015). However, for a regional study of aquifer capacity, the 3D numerical models are more suitable (Anderson et al., 2015; Okofo and Martienssen, 2022). Apart from the current set of parameters, the PARR value is also dependent on the other well parameters such as skin layer thickness, pipe length, friction coefficient, and screen slot dimension (which cause significant head losses during injection (Houben, 2015a; b) and can't be modelled in MODFLOW with available packages. The methodology presented here can be applied to different aquifer types and models to assess its robustness. The utilization of PARR in the assessment and design of ASR systems should be explored with the available window of surplus availability. Apart from this, the presented study assumes PARR as a constant recharge rate throughout the injection duration which can be inefficient to fully utilize the true aquifer storage capacity. To achieve this, the dynamic injection rate will be explored in future research.

6. Summary and conclusion

An adaptive algorithm-based optimization approach has been introduced to determine the novel metric Permissible Aquifer Recharge Rate (PARR) using numerical groundwater flow models. A detailed conceptualization of PARR has been presented, the factors affecting have been examined. The global sensitivity analysis of PARR to aquifer and well parameters have been presented using Sobol's indices. The methodology is demonstrated in France's Lower Ain River Basin, highlighting its potential application in aquifer storage and recovery (ASR) site selection.

The proposed methodology for the determination of PARR is crucial before planning artificial recharge through injection wells, as it provides the temporal variation of maximum achievable recharge rates at a site. PARR is a valuable tool for managed aquifer recharge site selection and recharge operation planning. The adaptive algorithm-based approach significantly reduces computational time, which is essential for iterative simulation-based frameworks involving numerical groundwater models. The sensitivity analysis presented in this research highlights that the interplay of aquifers and well parameters are more dominant in achieving the higher injection rates.

The specific conclusions of this research work are as follows:

1. The methodology for determining PARR with an adaptive iteration algorithm based on the analytical solution to the well is efficient and requires fewer iterations. The methodology can be extended to other problems which requires the determination of drawdown or head built-up, iteratively from a numerical model.
2. The combined effect of the location and size of the well screen on PARR suggests that the best location for the screen to be placed is near the bottom of the aquifer to get higher PARR.
3. The PARR is more sensitive to specific parameter interactions, particularly between hydraulic conductivity and vertical anisotropy in the case of an unconfined aquifer. This suggests that managing unconfined aquifers requires careful consideration of how these parameters interplay. In contrast, confined aquifers exhibit a more

distributed sensitivity across multiple parameters, indicating a broader range of factors influencing PARR.

4. The implementation of the methodology in the Lower Ain River Basin highlights the applicability and spatial variability of PARR influenced by the aquifer characteristics. The study suggests a strong aquifer storage potential of the Ain River Basin, which can be utilized in case of severe groundwater deficiency.

CRediT authorship contribution statement

Ranveer Kumar: Writing – original draft, Software, Methodology, Conceptualization. **Anurag Ohri:** Supervision. **Shishir Gaur:** Writing – review & editing, Conceptualization.

Declaration of competing interest

The authors declare that they have no known competing financial interests or personal relationships that could have appeared to influence the work reported in this paper.

Acknowledgements

The authors want to acknowledge the Prime Minister Research Fellowship granted to Ranveer Kumar in his PhD. The authors would also like to acknowledge Dr. Hervé Piégay and the joint Indian-French International Research Project (IRP-CNRS) on 'Effects of River-Aquifer Exchanges on Riverine Ecosystem Resilience to Global Change Comparative Approach of the Ganga and Rhône River Basin Networks' (2021–2026) for providing valuable data and model of Ain River Basin to implement the presented work. The authors sincerely appreciate the anonymous reviewers for their valuable suggestions.

Appendix

A. Global sensitivity analysis (GSA) with Sobol's indices.

Sensitivity analysis is an important part of scientific research and modelling because it helps researchers understand the relative relevance of numerous input variables in affecting the output of a complex system. Sobol's method (Sobol, 1993) is a global sensitivity analysis technique that quantifies each input variable's contribution to output variation while accounting for all interactions. It performs particularly well in complex, nonlinear models. The method uses variance decomposition to generate sensitivity indices, also known as Sobol's indices, for each input parameter. The decomposition of the total variance of the output Y to fractions is attributed to input variables and their interactions. For a model $Y = f(X_1, X_2, \ldots, X_k)$ with k input variables $X_1, X_2, \ldots, X_k$, the variance $Var(Y)$ can be decomposed as:

$$Var(\mathrm{Y}) = \sum_{\mathrm{i}=1}^{\mathrm{k}} \mathrm{V_i} + \sum_{1\le \mathrm{i}<\mathrm{j}\le \mathrm{k}} \mathrm{V_{ij}} + \sum_{1\le \mathrm{i}<\mathrm{j}<\mathrm{l}\le \mathrm{k}} \mathrm{V_{ijl}} + \cdots + \mathrm{V_{12\cdots k}}] \tag{A.1}$$

Where V_i is the variance contribution of the *i-th* input alone, V_{ij} is the contribution of the interaction between X_i and X_j, and further with other combinations of variables. The variance decomposition in Eq. (A.1) can be utilized to define the sensitivity indices of different orders as follows:

$$\mathrm{S_i} = \frac{\mathrm{V_i}}{\mathrm{Var(Y)}} \tag{A.2}$$

$$\mathrm{S_{ij}} = \frac{\mathrm{V_{ij}}}{\mathrm{Var(Y)}} \tag{A.3}$$

$$\mathrm{S_{Ti}} = 1 - \frac{V_{\sim \mathrm{i}}}{\mathrm{Var(Y)}} \tag{A.4}$$

Such that,

$$V_i = Var(\mathbb{E}[Y|X_i]) \tag{A.5}$$

$$V_{ij} = Var(\mathbb{E}[Y|X_i, X_j]) - V_i - V_j - V_{ijk} - \ldots \tag{A.6}$$

$$V_{\sim i} = Var(\mathbb{E}[Y|X_{\sim i}]) \tag{A.7}$$

Where S_i is the first-order Sobol index that measures the contribution of a single input variable X_i, to the output variance. S_{ij} is the second-order Sobol index that measures the contribution of interaction between variables X_i and X_j to the output variance. S_{Ti} is the total Sobol index that measures the contribution of interaction between variables X_i and X_j to the output variance. V_i is the variance of the conditional expectation ($\mathbb{E}$) of Y given X_i. V_{ij} is the variance of the conditional expectation of Y given X_i and X_j, excluding first-order and higher-order interactions. $V_{\sim \mathrm{i}}$ is the variance of the conditional expectation of Y given all variables except X_i.

The original Sobol's method, used for sensitivity analysis, required $n \times (2\,m + 1)$ model runs to estimate sensitivity indices, where n is the sample size, and m is the number of parameters. To improve this method, (Saltelli, 2002) developed an enhanced version that can compute the first, second, and total order sensitivity indices using $n \times (2\,m + 2)$ model runs. This enhancement ensures a quasi-random, space-filling sampling strategy, improving the estimation of higher-order interactions. In this study, we employed Saltelli sampling with a base sample size of 1,024, resulting in 14,336 model evaluations for six parameters, ensuring a robust exploration of parameter interactions and variance contributions.

Data availability

Data will be made available on request.

References

Agarwal, R.G., Al-Hussainy, R., Ramey, H.J., 1970. An investigation of wellbore storage and skin effect in unsteady liquid flow: I. Analytical treatment. Soc. Pet. Eng. J. 10, 279–290. https://doi.org/10.2118/2466-PA.

Alam, S., Borthakur, A., Ravi, S., Gebremichael, M., Mohanty, S.K., 2021. Managed aquifer recharge implementation criteria to achieve water sustainability. Sci. Total Environ. 768, 144992. https://doi.org/10.1016/j.scitotenv.2021.144992.
Anderson, M.G., Woessner, W.W., Hunt, R.J., 2015. Applied Groundwater Modeling: Simulation of Flow and Advective Transport, second ed. Elsevier.
Andrews, C.B., 2008. Effective groundwater model calibration: with analysis of data, sensitivities, predictions, and uncertainty. Groundwater 46, 5. https://doi.org/10.1111/j.1745-6584.2007.00398.x.
Atawneh, D.Al, Cartwright, N., Bertone, E., 2021. Climate change and its impact on the projected values of groundwater recharge: A review. Journal of Hydrology 601, 126602. https://doi.org/10.1016/j.jhydrol.2021.126602.
Bajpai, M., Gaur, S., Kumar, R., Ohri, A., Piégay, H., 2023. Suitable sites for groundwater development: a capture map-based approach integrated with weighted overlay analysis. AQUA — Water Infrastruct. Ecosyst Soc. 72, 1184–1197. https://doi.org/10.2166/aqua.2023.011.
Baker, E.A., Cappato, A., Todeschini, S., Tamellini, L., Sangalli, G., Reali, A., Manenti, S., 2022. Combining the Morris method and multiple error metrics to assess aquifer characteristics and recharge in the lower Ticino Basin, in Italy. J. Hydrol. (Amst) 614, 128536. https://doi.org/10.1016/j.jhydrol.2022.128536.
Baker, E.A., Manenti, S., Reali, A., Sangalli, G., Tamellini, L., Todeschini, S., 2023. Combining noisy well data and expert knowledge in a Bayesian calibration of a flow model under uncertainties: an application to solute transport in the Ticino basin. GEM 14, 8. https://doi.org/10.1007/s13137-023-00219-8.
Barlow, P.M., Moench, A.F. 1999. WTAQ–A computer program for calculating drawdowns and estimating hydraulic properties for confined and water-table aquifers: U.S. Geological Survey Water-Resources Investigations Report.
Bergmo, P.E.S., Grimstad, A.-A., Lindeberg, E., 2011. Simultaneous CO_2 injection and water production to optimise aquifer storage capacity. Int. J. Greenhouse Gas Control 5, 555–564. https://doi.org/10.1016/j.ijggc.2010.09.002.
Bianchi Janetti, E., Guadagnini, L., Riva, M., Guadagnini, A., 2019. Global sensitivity analyses of multiple conceptual models with uncertain parameters driving groundwater flow in a regional-scale sedimentary aquifer. J. Hydrol. (Amst) 574, 544–556. https://doi.org/10.1016/j.jhydrol.2019.04.035.
Briggs, A., Sculpher, M., Buxton, M., 1994. Uncertainty in the economic evaluation of health care technologies: the role of sensitivity analysis. Health Econ. 3, 95–104. https://doi.org/10.1002/hec.4730030206.
Chahar, B.R., 2015. Groundwater Hydrology. McGraw Hill Education (India) Private Limited, New Delhi.
Corne, R. 2023. A comparison analysis: the 2022 drought on the Rhone and the Po basins. POLITECNICO DI TORINO.
Dillon, P., Stuyfzand, P., Grischek, T., Lluria, M., Pyne, R.D.G., Jain, R.C., Bear, J., Schwarz, J., Wang, W., Fernandez, E., Stefan, C., Pettenati, M., van der Gun, J., Sprenger, C., Massmann, G., Scanlon, B.R., Xanke, J., Jokela, P., Zheng, Y., Rossetto, R., Shamrukh, M., Pavelic, P., Murray, E., Ross, A., Bonilla Valverde, J.P., Palma Nava, A., Ansems, N., Posavec, K., Ha, K., Martin, R., Sapiano, M., 2019. Sixty years of global progress in managed aquifer recharge. Hydrogeol. J. 27, 1–30. https://doi.org/10.1007/s10040-018-1841-z.
Dillon, P.J., Hickinbotham, M.R., Pavelic, P., 1994. Review of international experience in injecting water into aquifers for storage and reuse. In: Water down under 94: Groundwater Papers; Preprints of Papers. Institution of Engineers, Australia Barton, ACT, pp. 13–14.
Freeze, R.A., Cherry, J.A., 1979. Groundwater. Prentice-Hall International, London.
Freeze, R.A., Witherspoon, P.A., 1966. Theoretical analysis of regional groundwater flow: 1. Analytical and numerical solutions to the mathematical model. Water Resour Res 2, 641–656. https://doi.org/10.1029/WR002i004p00641.
Gan, Y., Duan, Q., Gong, W., Tong, C., Sun, Y., Chu, W., Ye, A., Miao, C., Di, Z., 2014. A comprehensive evaluation of various sensitivity analysis methods: a case study with a hydrological model. Environ. Model. Softw. 51, 269–285. https://doi.org/10.1016/j.envsoft.2013.09.031.
Gaur, S., Chahar, B.R., Graillot, D., 2011. Analytic elements method and particle swarm optimization based simulation-optimization model for groundwater management. J. Hydrol. (Amst) 402, 217–227. https://doi.org/10.1016/j.jhydrol.2011.03.016.
Gaur, S., Kumar, R., Ohri, A., Mishra, S., Gond, A.K., Dwivedi, S.B., Jha, M., Chaturvedi, A., Singh, B.N., 2023. Study of hydrologically critical subbasins under climate change. J. Water Clim. Change 14, 1723–1740. https://doi.org/10.2166/wcc.2023.038.
Graillot, D., Paran, F., Bornette, G., Marmonier, P., Piscart, C., Cadilhac, L., 2014. Coupling groundwater modeling and biological indicators for identifying river/aquifer exchanges. Springerplus 3, 1–14. https://doi.org/10.1186/2193-1801-3-68.
Hantush, M.S. 1964. Hydraulics of Wells. pp. 281–432. https://doi.org/10.1016/B978-1-4831-9932-0.50010-3.
Herman, J., Usher, W., 2017. SALib: an open-source python library for sensitivity. Analysis 41, 9–10. https://doi.org/10.1016/S0010-1.
Houben, G.J., 2015a. Review: hydraulics of water wells—flow laws and influence of geometry. Hydrogeol. J. 23, 1633–1657. https://doi.org/10.1007/s10040-015-1312-8.
Houben, Georg J, 2015. Review: Hydraulics of water wells — head losses of individual components 1659–1675. https://doi.org/10.1007/s10040-015-1313-7.
Huang, C.-S., Tsai, Y.-H., Yeh, H.-D., Yang, T., 2019. A general analytical model for head response to oscillatory pumping in unconfined aquifers: effects of delayed gravity drainage and initial condition. Hydrol. Earth Syst. Sci. 23, 1323–1337. https://doi.org/10.5194/hess-23-1323-2019.
Hugman, R., Stigter, T.Y., Monteiro, J.P., Nunes, L., 2012. Influence of aquifer properties and the spatial and temporal distribution of recharge and abstraction on sustainable yields in semi-arid regions. Hydrol. Process. 26, 2791–2801. https://doi.org/10.1002/hyp.8353.
Jenkins, L.T., Foschi, M., MacMinn, C.W., 2019. Impact of pressure dissipation on fluid injection into layered aquifers. J. Fluid Mech. 877, 214–238. https://doi.org/10.1017/jfm.2019.593.
Kuiper, L.K., 1983. A numerical procedure for the solution of the steady state variable density groundwater flow equation. Water Resour. Res. 19, 234–240. https://doi.org/10.1029/WR019i001p00234.
Kumar, R., Gaur, S., Soni, P., Maurya, P., Ohri, A., 2024a. HRU-based downscaling of GRACE-TWS to quantify the hydrogeological fluxes and specific yield in the lower middle ganga basin. J. Hydrol. (Amst) 639, 131591. https://doi.org/10.1016/j.jhydrol.2024.131591.
Kumar, R., Tewari, A., Mishra, S., Singh, P.K., Gaur, S., 2024b. Multi-Facet analysis of analytical and numerical models to resolve sustainable artificial recharge rates in unconfined aquifers. J. Environ. Manage. 362, 121233. https://doi.org/10.1016/j.jenvman.2024.121233.
Lejot, J., Delacourt, C., Piégay, H., Fournier, T., Trémélo, M.-L., Allemand, P., 2007. Very high spatial resolution imagery for channel bathymetry and topography from an unmanned mapping controlled platform. Earth Surf. Process. Landf. 32, 1705–1725. https://doi.org/10.1002/esp.1595.
Leonard, F., Konikow, George Z. Hornberger, Keith J. Halford, R.T.H., 2009. Revised Multi-Node Well (MNW2) Package for MODFLOW Ground-Water Flow Model Techniques and Methods 6 – A30. Methods 80.
Li, J., Chen, J.J., Li, M.G., Xia, X.H., 2020. Well hydraulics of temporally varying artificial recharge with well clogging in confined aquifers. Arab. J. Geosci. 13. https://doi.org/10.1007/s12517-020-05898-3.
Martinez, M.B., Widdowson, M.A., 2023. Evaluating flow distribution in a multiaquifer recharge well using an in situ flowmeter. Groundwater. https://doi.org/10.1111/gwat.13379.
Mishra, S., Bosc, L., Gaur, S., Kacem, M., Ohri, A., 2023. Handling large decision variables in multi-objective groundwater optimization problems: aquifer parameter-based clustering approach. Water Resour. Manag. 37, 4553–4568. https://doi.org/10.1007/s11269-023-03580-3.
Moench, A.F., 1997. Flow to a well of finite diameter in a homogeneous, anisotropic water table aquifer. Water Resour. Res. 33, 1397–1407. https://doi.org/10.1029/97WR00651.
Myoung-Rak, C., Jang-Hwan, C., Gyoo-Bum, K., 2020. Preliminary Assessment of Groundwater Artificial Recharge Effect Using a Numerical Model at a Small Basin. 지질공학 30, 269–278. https://doi.org/10.9720/KSEG.2020.3.269.
Nättorp, A., Brand, J., Chadha, D.K., Elango, L., Ghosh, N.C., Grützmacher, G., Sprenger, C., Kumar, S., 2016. Overview of managed aquifer recharge in India. Natural Water Treatment Systems for Safe and Sustainable Water Supply in the Indian Context: Saph Pani 79.
Neuman, S.P., 1972. Theory of flow in unconfined aquifers considering delayed response of the water table. Water Resour. Res. 8, 1031–1045. https://doi.org/10.1029/WR008i004p01031.
Nossent, J., Elsen, P., Bauwens, W., 2011. Sobol' sensitivity analysis of a complex environmental model. Environ. Model. Softw. 26, 1515–1525. https://doi.org/10.1016/j.envsoft.2011.08.010.
Okofo, L.B., Martienssen, M., 2022. A three-dimensional numerical groundwater flow model to assess the feasibility of managed aquifer recharge in the Tamne River basin of Ghana. Hydrogeol. J. 30, 1071–1090. https://doi.org/10.1007/s10040-022-02492-7.
Olivier, J., Olivier, J., Cedex, P., Cedex, V., Malard, F. 2009. The Rhˆone River Basin. https://doi.org/10.1016/B978-0-12-369449-2.00007-2.
Parker, T.K., Jansen, J., Behroozmand, A.A., Halkjaer, M., Thorn, P., 2022. Applied geophysics for managed aquifer recharge. Groundwater 60, 606–618. https://doi.org/10.1111/gwat.13235.
Pyne, R.D.G., 2017. In: Groundwater Recharge and Wells. CRC Press. https://doi.org/10.1201/9780203719718.
Reinecke, R., Foglia, L., Mehl, S., Herman, J.D., Wachholz, A., Trautmann, T., Döll, P., 2019. Spatially distributed sensitivity of simulated global groundwater heads and flows to hydraulic conductivity, groundwater recharge, and surface water body parameterization. Hydrol. Earth Syst. Sci. 23, 4561–4582. https://doi.org/10.5194/hess-23-4561-2019.
Ruder, S. 2017. An overview of gradient descent optimization algorithms.
Rushton, K.R., Srivastava, N.K., 1988. Interpreting injection well tests in an alluvial aquifer. J. Hydrol. (Amst) 99, 49–60. https://doi.org/10.1016/0022-1694(88)90077-7.
Saltelli, A., 2002. Making best use of model evaluations to compute sensitivity indices. Comput. Phys. Commun. 145, 280–297. https://doi.org/10.1016/S0010-4655(02)00280-1.
Schiff, L., 1964. Ground-water recharge hydrology. Groundwater 2, 16–20. https://doi.org/10.1111/j.1745-6584.1964.tb01766.x.
Schwartz, F.W., Ibaraki, M., 2011. Groundwater: a resource in decline. Elements 7, 175–179. https://doi.org/10.2113/gselements.7.3.175.
Shandilya, R.N., Bresciani, E., Kang, P.K., Lee, S., 2022a. Influence of hydrogeological and operational parameters on well pumping capacity. J. Hydrol. (Amst) 608, 127643. https://doi.org/10.1016/j.jhydrol.2022.127643.
Shandilya, R.N., Bresciani, E., Runkel, A.C., Jennings, C.E., Lee, S., Kang, P.K., 2022b. Aquifer-scale mapping of injection capacity for potential aquifer storage and recovery sites: methodology development and case studies in Minnesota, USA. J. Hydrol. Reg. Stud. 40, 101048. https://doi.org/10.1016/j.ejrh.2022.101048.
Sobol, I.M. 1993. Sensitivity Estimates for Nonlinear Mathematical Models.
Song, X., Zhang, J., Zhan, C., Xuan, Y., Ye, M., Xu, C., 2015. Global sensitivity analysis in hydrological modeling: review of concepts, methods, theoretical framework, and applications. J. Hydrol. (Amst) 523, 739–757. https://doi.org/10.1016/j.jhydrol.2015.02.013.

Sprenger, C., Hartog, N., Hernández, M., Vilanova, E., Grützmacher, G., Scheibler, F., Hannappel, S., 2017. Inventaire des sites de gestion des aquifères par recharge en Europe: développement historique, situation actuelle et perspectives. Hydrogeol. J. 25, 1909–1922. https://doi.org/10.1007/s10040-017-1554-8.

Sun, X., Xiang, Y., Shi, Z., 2018. Estimating the hydraulic parameters of a confined aquifer based on the response of groundwater levels to seismic Rayleigh waves. Geophys. J. Int. 213, 919–930. https://doi.org/10.1093/gji/ggy036.

Tang, Y., Reed, P., Wagener, T., Van Werkhoven, K., 2007. Comparing sensitivity analysis methods to advance lumped watershed model identification and evaluation. Hydrol. Earth Syst. Sci. 11, 793–817. https://doi.org/10.5194/hess-11-793-2007.

Tewari, A., Singh, P.K., Gaur, S., Mishra, S., Kumar, R., 2023. Cluster-based delineation of optimal sites for managed aquifer recharge: a case study of Lower Betwa River Basin, India. Environ. Earth Sci. 83, 20. https://doi.org/10.1007/s12665-023-11308-0.

Theis, C.V., 1935. The relation between the lowering of the Piezometric surface and the rate and duration of discharge of a well using ground-water storage. Eos Trans. AGU 16, 519–524. https://doi.org/10.1029/TR016i002p00519.

Tholeti, T., Kalyani, S., 2020. Tune smarter not harder: a principled approach to tuning learning rates for shallow nets. IEEE Trans. Signal Process. 68, 5063–5078. https://doi.org/10.1109/TSP.2020.3019655.

Tiwari, S., Yadav, B.K., 2024. Role of hydrogeological factors on aquifer storage and recovery performance in saline groundwater regions. J. Water Resour. Plan Manag. 150, 1–11. https://doi.org/10.1061/jwrmd5.wreng-5949.

Van Everdingen, A.F., 1953. The skin effect and its influence on the productive capacity of a well. J. Petrol. Tech. 5, 171–176. https://doi.org/10.2118/203-G.

van Lopik, J.H., Sweijen, T., Hartog, N., Schotting, R.J., 2021. Contribution to head loss by partial penetration and well completion: implications for dewatering and artificial recharge wells. Hydrogeol. J. 29, 875–893. https://doi.org/10.1007/s10040-020-02228-5.

Vergnes, J.P., Caballero, Y., Lanini, S., 2023. Assessing climate change impact on French groundwater resources using a spatially distributed hydrogeological model. Hydrol. Sci. J. 68, 209–227. https://doi.org/10.1080/02626667.2022.2150553.

Wang, X., Luo, J., 2021. General analytical solutions of groundwater flow toward multi-dimensional sources/sinks in a confined aquifer with leakage and distributed recharge. J. Hydrol. (Amst) 594, 125948. https://doi.org/10.1016/j.jhydrol.2020.125948.

Welch, C., Cook, P.G., Harrington, G.A., Robinson, N.I., 2013. Propagation of solutes and pressure into aquifers following river stage rise. Water Resour. Res. 49, 5246–5259. https://doi.org/10.1002/wrcr.20408.

Zeiler, M.D. 2012. ADADELTA: An Adaptive Learning Rate Method.